Biomedical Optics EXPRESS

Optical coherence tomography-based parameterization and quantification of articular cartilage surface integrity

Nicolai Brill,[1,*] Jörn Riedel,[1] Björn Rath,[2] Markus Tingart,[2] Holger Jahr,[2] Marcel Betsch,[2] Valentin Quack,[2] Thomas Pufe,[3] Robert Schmitt,[1,4] and Sven Nebelung[2,3]

[1]*Fraunhofer Institute for Production Technology, Aachen, Germany*
[2]*Department of Orthopaedic Surgery, Aachen University Hospital, Aachen, Germany*
[3]*Institute of Anatomy and Cell Biology, RWTH Aachen, Aachen, Germany*
[4]*Laboratory for Machine Tools and Production Engineering, RWTH Aachen, Aachen, Germany*
**Nicolai.Brill@ipt.fraunhofer.de*

Abstract: Loss of articular cartilage surface integrity is considered the earliest sign of osteoarthritis; however, its reliable detection has not been established by clinical routine diagnostics. This study comprehensively assesses a set of 11 algorithm-based 2-D Optical Coherence Tomography roughness parameters and investigates their clinical impact. Histology and manual irregularity quantification of 105 human cartilage samples with variable degeneration served as reference. The majority of parameters revealed a close-to-linear correlation with the entire spectrum of degeneration. Surface integrity should therefore be assessed by a combination of parameters to improve current diagnostic accuracy in the determination of cartilage degeneration.

OCIS codes: (170.6935) Tissue characterization; (170.3880) Medical and biological imaging; (170.1610) Clinical applications; (170.4500) Optical coherence tomography.

References and links

1. R. W. Moskowitz, "The burden of osteoarthritis: clinical and quality-of-life issues," Am. J. Manag. Care **15**(8 Suppl), S223–S229 (2009).
2. K. P. Pritzker, S. Gay, S. A. Jimenez, K. Ostergaard, J. P. Pelletier, P. A. Revell, D. Salter, and W. B. van den Berg, "Osteoarthritis cartilage histopathology: grading and staging," Osteoarthritis Cartilage **14**(1), 13–29 (2006).
3. H. E. Panula, M. M. Hyttinen, J. P. Arokoski, T. K. Långsjö, A. Pelttari, I. Kiviranta, and H. J. Helminen, "Articular cartilage superficial zone collagen birefringence reduced and cartilage thickness increased before surface fibrillation in experimental osteoarthritis," Ann. Rheum. Dis. **57**(4), 237–245 (1998).
4. J. A. Buckwalter and H. J. Mankin, "Articular cartilage: degeneration and osteoarthritis, repair, regeneration, and transplantation," Instr. Course Lect. **47**, 487–504 (1998).
5. A. C. Bay-Jensen, S. Hoegh-Madsen, E. Dam, K. Henriksen, B. C. Sondergaard, P. Pastoureau, P. Qvist, and M. A. Karsdal, "Which elements are involved in reversible and irreversible cartilage degradation in osteoarthritis?" Rheumatol. Int. **30**(4), 435–442 (2010).
6. B. J. Moa-Anderson, K. D. Costa, C. T. Hung, and G. A. Ateshian, "Bovine articular cartilage surface topography and roughness in fresh versus frozen tissue samples using atomic force microscopy.," in Summer Bioengineering Conference., (Key Biscayne, Florida, 2003).
7. P. A. Smyth, R. E. Rifkin, R. L. Jackson, and R. R. Hanson, "A surface roughness comparison of cartilage in different types of synovial joints," J. Biomech. Eng. **134**(2), 021006 (2012).
8. H. Forster and J. Fisher, "The influence of continuous sliding and subsequent surface wear on the friction of articular cartilage," Proc. Inst. Mech. Eng. H **213**(4), 329–345 (1999).
9. R. D. Bloebaum and K. M. Radley, "Three-dimensional surface analysis of young adult human articular cartilage," J. Anat. **187**(Pt 2), 293–301 (1995).
10. S. Saarakkala, M. S. Laasanen, J. S. Jurvelin, and J. Töyräs, "Quantitative ultrasound imaging detects degenerative changes in articular cartilage surface and subchondral bone," Phys. Med. Biol. **51**(20), 5333–5346 (2006).

#236329 - $15.00 USD Received 16 Mar 2015; revised 18 May 2015; accepted 19 May 2015; published 8 Jun 2015

11. S. Ghosh, J. Bowen, K. Jiang, D. M. Espino, and D. E. Shepherd, "Investigation of techniques for the measurement of articular cartilage surface roughness," Micron **44**, 179–184 (2013).
12. W. Krampla, M. Roesel, K. Svoboda, A. Nachbagauer, M. Gschwantler, and W. Hruby, "MRI of the knee: how do field strength and radiologist's experience influence diagnostic accuracy and interobserver correlation in assessing chondral and meniscal lesions and the integrity of the anterior cruciate ligament?" Eur. Radiol. **19**(6), 1519–1528 (2009).
13. C. R. Chu, D. Lin, J. L. Geisler, C. T. Chu, F. H. Fu, and Y. Pan, "Arthroscopic microscopy of articular cartilage using optical coherence tomography," Am. J. Sports Med. **32**(3), 699–709 (2004).
14. X. Li, S. Martin, C. Pitris, R. Ghanta, D. L. Stamper, M. Harman, J. G. Fujimoto, and M. E. Brezinski, "High-resolution optical coherence tomographic imaging of osteoarthritic cartilage during open knee surgery," Arthritis Res. Ther. **7**(2), R318–R323 (2005).
15. T. Xie, S. Guo, J. Zhang, Z. Chen, and G. M. Peavy, "Determination of characteristics of degenerative joint disease using optical coherence tomography and polarization sensitive optical coherence tomography," Lasers Surg. Med. **38**(9), 852–865 (2006).
16. T. Virén, Y. P. Huang, S. Saarakkala, H. Pulkkinen, V. Tiitu, A. Linjama, I. Kiviranta, M. J. Lammi, A. Brünott, H. Brommer, R. Van Weeren, P. A. Brama, Y. P. Zheng, J. S. Jurvelin, and J. Töyräs, "Comparison of ultrasound and optical coherence tomography techniques for evaluation of integrity of spontaneously repaired horse cartilage," J. Med. Eng. Technol. **36**(3), 185–192 (2012).
17. S. Saarakkala, S. Z. Wang, Y. P. Huang, and Y. P. Zheng, "Quantification of the optical surface reflection and surface roughness of articular cartilage using optical coherence tomography," Phys. Med. Biol. **54**(22), 6837–6852 (2009).
18. S. Nebelung, U. Marx, N. Brill, D. Arbab, V. Quack, H. Jahr, M. Tingart, B. Zhou, M. Stoffel, R. Schmitt, and B. Rath, "Morphometric grading of osteoarthritis by optical coherence tomography--an ex vivo study," J. Orthop. Res. **32**(10), 1381–1388 (2014).
19. P. Cernohorsky, A. C. Kok, D. M. Bruin, M. J. Brandt, D. J. Faber, G. J. Tuijthof, G. M. Kerkhoffs, S. D. Strackee, and T. G. van Leeuwen, "Comparison of optical coherence tomography and histopathology in quantitative assessment of goat talus articular cartilage," Acta Orthop. **86**(2), 257–263 (2015).
20. Y. P. Huang, S. Saarakkala, J. Toyras, L. K. Wang, J. S. Jurvelin, and Y. P. Zheng, "Effects of optical beam angle on quantitative optical coherence tomography (OCT) in normal and surface degenerated bovine articular cartilage," Phys. Med. Biol. **56**(2), 491–509 (2011).
21. M. Terukina, H. Fujioka, S. Yoshiya, M. Kurosaka, T. Makino, N. Matsui, and J. Tanaka, "Analysis of the thickness and curvature of articular cartilage of the femoral condyle," Arthroscopy **19**(9), 969–973 (2003).
22. U. Marx, R. Schmitt, S. Nebelung, M. Tingart, C. Luring, and B. Rath, "In-vitro observation of cartilage-degeneration progression by Fourier-domain OCT," in Advanced Biomedical and Clinical Diagnostic Systems, T. Vo-Dinh, ed. (Society of Photo-Optical Instrumentation Engineers -SPIE-, San Francisco, California, United States, 2012), pp. 1–7.
23. Z. Peng and M. Wang, "Three dimensional surface characterization of human cartilages at a micron and nanometre scale," Wear **301**(1-2), 210–217 (2013).
24. H. J. Mankin, H. Dorfman, L. Lippiello, and A. Zarins, "Biochemical and metabolic abnormalities in articular cartilage from osteo-arthritic human hips. II. Correlation of morphology with biochemical and metabolic data," J. Bone Joint Surg. Am. **53**(3), 523–537 (1971).
25. B. L. Wong, W. C. Bae, J. Chun, K. R. Gratz, M. Lotz, and R. L. Sah, "Biomechanics of cartilage articulation: effects of lubrication and degeneration on shear deformation," Arthritis Rheum. **58**(7), 2065–2074 (2008).
26. R. U. Kleemann, D. Krocker, A. Cedraro, J. Tuischer, and G. N. Duda, "Altered cartilage mechanics and histology in knee osteoarthritis: relation to clinical assessment (ICRS Grade)," Osteoarthritis Cartilage **13**(11), 958–963 (2005).
27. J. Meister, R. Franzen, K. Gavenis, M. Zaum, S. Stanzel, N. Gutknecht, and B. Schmidt-Rohlfing, "Ablation of articular cartilage with an erbium:YAG laser: an ex vivo study using porcine models under real conditions-ablation measurement and histological examination," Lasers Surg. Med. **41**(9), 674–685 (2009).
28. G. R. Squires, S. Okouneff, M. Ionescu, and A. R. Poole, "The pathobiology of focal lesion development in aging human articular cartilage and molecular matrix changes characteristic of osteoarthritis," Arthritis Rheum. **48**(5), 1261–1270 (2003).
29. S. Nebelung, N. Brill, U. Marx, V. Quack, M. Tingart, R. Schmitt, B. Rath, and H. Jahr, "Three-dimensional imaging and analysis of human cartilage degeneration using Optical Coherence Tomography," J. Orthop. Res. **33**(5), 651–659 (2015).
30. P. H. Puhakka, J. H. Ylärinne, M. J. Lammi, S. Saarakkala, V. Tiitu, H. Kröger, T. Virén, J. S. Jurvelin, and J. Töyräs, "Dependence of light attenuation and backscattering on collagen concentration and chondrocyte density in agarose scaffolds," Phys. Med. Biol. **59**(21), 6537–6548 (2014).
31. D. M. Bear, M. Szczodry, S. Kramer, C. H. Coyle, P. Smolinski, and C. R. Chu, "Optical coherence tomography detection of subclinical traumatic cartilage injury," J. Orthop. Trauma **24**(9), 577–582 (2010).
32. D. K. Kasaragod, Z. Lu, and S. J. Matcher, "Comparative study of the angle-resolved backscattering properties of collagen fibers in bovine tendon and cartilage," J. Biomed. Opt. **16**(8), 080501 (2011).
33. V. Jaedicke, S. Agcaer, F. E. Robles, M. Steinert, D. Jones, S. Goebel, N. C. Gerhardt, H. Welp, and M. R. Hofmann, "Comparison of different metrics for analysis and visualization in spectroscopic optical coherence tomography," Biomed. Opt. Express **4**(12), 2945–2961 (2013).

#236329 - $15.00 USD Received 16 Mar 2015; revised 18 May 2015; accepted 19 May 2015; published 8 Jun 2015

1. Introduction

Articular cartilage lines the surface of synovial joints and facilitates joint movement due to its role in load transmission and maintenance of low friction. Osteoarthritis (OA), i.e. cartilage degeneration, is an important cause of disability in humans with great medical and socioeconomic implications [1]. Early diagnosis and treatment are, therefore, clinically highly relevant.

Degeneration is marked by distinctive morphological and functional changes, with the superficial cartilage layer affected first in terms of proteoglycan depletion and alterations in collagen orientation, content and integrity [2–4]. Hence, earliest alterations include surface irregularity formation, erosion and fissuring. With preventive strategies available to modify joint biomechanics by surgical interventions or to improve tissue resilience by pharmaceutical agents, the very earliest evidence of degeneration must be detected and adequately addressed. Early detection of degeneration is crucial as the pathology may be reversible at this point [5].

Naturally, cartilage surface irregularities provide a target for imaging strategies. In the past, a variety of contact and non-contact methods have been used to determine articular cartilage surface roughness. Atomic force microscopy [6], stylus surface profilometry [7] or talysurf techniques [8] are contact methods that have been used on cartilage; however, their in-vivo use is limited, either due to handling issues or the possibility of technique-induced tissue deformation and measurement distortion. Non-contacting methods include laser profilometry [8], scanning electron microscopy stereoscopic imaging [9] and ultrasound [10]. Despite promising results, in-vivo applicability, practicality and resolution requirements have limited their clinical use [11]. Moreover, routinely used clinical imaging modalities such as X-ray, morphological MRI or arthroscopy are deficient in terms of either resolution, inter-observer reliability or sensitivity/specificity [12, 13].

Optical Coherence Tomography (OCT) is a new imaging modality that may close this diagnostic gap. As a light-based, high resolution, real time, non-invasive and non-destructive imaging modality, OCT is based on the detection of echo time delays and intensities of backscattered light. Similar to low power histology, modern OCT systems allow imaging at micrometer resolutions and to millimeter depths. The diagnostic value of OCT-based imaging was demonstrated in vitro and in vivo and in the context of open and arthroscopic knee surgery [13–15]. Lately, quantitative OCT-based image analysis and quantification of morphologic and optical parameters aimed at the more objective and reliable assessment of cartilage degeneration [16–18]. In particular, different approaches to determine surface roughness have been suggested and validated on human and non-human cartilage [13, 16–18].

OCT-based cartilage roughness measures as introduced by other investigators [13, 17] may be prone to inaccuracy when it comes to the definition of the idealized / mean smoothed surface that is used for reference purposes and roughness determination. In these studies, referencing is performed either to a line drawn by hand to simulate an ideally debrided smooth surface [13], to a semi-automatically determined auxiliary line that is constructed by manual surface point definition and subsequent interpolation [19] or to an averaged surface position [16, 20]. In the light of clinical needs, these approaches seem impractical as they require user input for reference line definition or may be inaccurate when used in situ or in vivo as human femoral condyle articular cartilage is characterized by considerable curvature (mean: 4.4 m^{-1}; range: –20.0 m^{-1}, 27.2 m^{-1}) [21], which could be challenging for techniques based on surface position averaging. Also, the latter approach has been demonstrated to be highly sensitive to non-perpendicularity of the OCT beam to the cartilage surface [20] which may introduce further inaccuracy in the actual surgical setting. Although our group recently reported a good correlation between OCT-based surface assessment and histological grading [18], the standard of OCT-based surface evaluation remains to be defined. Therefore, the objective of the present study was to comparatively evaluate a multitude of common 2-D roughness parameters and to assess their diagnostic value in different degrees of human

#236329 - $15.00 USD Received 16 Mar 2015; revised 18 May 2015; accepted 19 May 2015; published 8 Jun 2015

cartilage degeneration in an effort to realize the unequivocal image-based differentiation between healthy and degenerative cartilage. This study's hypothesis was that the comprehensive use of common surface profile 2-D parameters would improve OCT-based detection of structural cartilage degeneration.

2. Materials and methods

In total, 105 cartilage samples of different degenerative stages were obtained for this study, comprising a subgroup of an earlier reported study [18], i.e. 'bare bone' cartilage samples were excluded for the present study. As described previously [18], a total of 20 patients (6 male, 14 female; mean age 71.9 years [range 48 - 83 years]) undergoing total knee replacement due to severe primary osteoarthritis of the knee were included; appropriate informed patient consent and review board approval were obtained accordingly. Samples were harvested from the medial / lateral femoral condyle [n = 18 / n = 46] and the medial / lateral tibial plateau [n = 14 / n = 27]. Upon sterile excision during surgery, samples were collected in saline, transferred to the laboratory, kept refrigerated and cut to standard size (width x length x depth: 15 x 15 x 10 [mm]) with special care taken to create plain surface samples. Tissue marking dye (Polysciences, Warrington, US) spots at 8 mm apart defined the main imaging plane. For OCT measurements, a spectral-domain OCT device (Thorlabs, Dachau, Germany; superluminescent diode: 1325 nm; bandwidth: 150 nm; axial resolution: 7.5 µm in air; lateral resolution: 15 µm) as published before [18, 22] was used. Light beam angle perpendicularity was sought and samples aligned along the imaging plane before the central 2-D OCT scan was obtained and saved for image processing. Data pre-processing included fixed-pattern noise removal, spectral shaping and λ-to-κ interpolation. Afterwards, the Fourier transformation was calculated and displayed as an A-scan. Adjustments in brightness, contrast and gamma-values were performed once to reduce ghost images and artefacts. These adjustments were kept constant for all subsequent measurements. Morphological filtering of dilation and erosion reduced speckling and smaller artefacts, while transformation to binary data allowed subsequent surface identification by processing each A-scan and detecting the first pixel unequal to zero. The threshold value to get the binary image was calculated dynamically. For every image an auto-threshold value was calculated based on a clustering method. The two-dimensional actual surface profile thus detected ("primary profile") was then processed using established industrial roughness algorithms for technical surfaces as standardized in a series of ISO standards (EN ISO 4287, 4288, 11562, 12085, 13565). The primary profile was filtered with a high-pass Gaussian filter to remove waviness brought about by the overall more or less convex shape of the cartilage samples. The filter cut-off wavelength λ_c is defined in EN ISO 4288 in relation to the resulting roughness. In line with the expected absolute roughness values and the requirements of EN ISO 4288 filter cut-offs of λ_c = 800 µm and λ_c = 2500 µm were suitable to center the primary profile on zero and to remove any long-wavelength waviness so that only local structures remained ("roughness profile"). As the filter cut-off had a significant influence on the roughness parameters, its choice had to be well considered. Of note, the shape and the minimum and maximum depths and heights of the subsequent roughness profile varied significantly with different filtering parameters (Fig. 1).

#236329 - $15.00 USD Received 16 Mar 2015; revised 18 May 2015; accepted 19 May 2015; published 8 Jun 2015

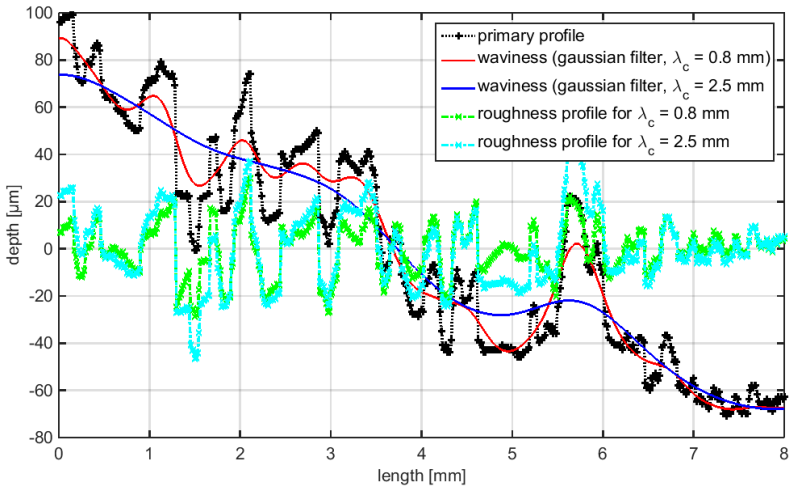

Fig. 1. Calculation of the roughness profile from a primary profile as exemplified by a moderate-to-severely diseased cartilage sample; notice the difference in the resulting roughness profiles when using different filter cut-off wavelengths. In the present study, a filter cut-off wavelength of λ_c = 800 µm as defined by EN ISO 4288 was used.

Longer cut-off wavelengths increase the impact of rough surface features, whereas shorter cut-off wavelengths increase the weight of small features. The cartilage irregularities to be quantified, in particular early and very early stages of disease, were most likely to constitute short-wavelengths features found at shorter wavelengths [23]. Therefore, a short filter wavelength was considered to be beneficial and a cut-off of λ_c = 800 µm was applied. Overall, this filtering routine was performed automatically without any user input except for the one-time definition of the filter wavelength λ_c. The roughness profile thus obtained was used for the calculation of the 2-D roughness parameters. From the wide variety of parameters listed in the ISO norm, a representative set of 11 parameters focusing on different profile characteristics was selected. For roughness profiles, the mean line used for reference purposes is the zero line. Overall, roughness parameters were grouped according to their theoretical conception into:

average of ordinates parameters

- R_a (arithmetical mean deviation of roughness profile / first moment) is the arithmetic mean of the absolute deviations from the mean line and is calculated (Eq. (1);

$$R_a = \frac{1}{l}\int_0^l |z(x)|\,dx \tag{1}$$

- R_q (root mean square deviation of roughness profile / second moment) is the root mean square of the absolute deviations from the mean line and is calculated (Eq. (2); this parameter is similar to the *Optical Roughness Index* [16, 20] and the *Fibrillation Index* [13] as published before with the main difference in the choice of the base waviness profile;

$$R_q = \sqrt{\frac{1}{l}\int_0^l |z^2(x)|\,dx} \tag{2}$$

#236329 - $15.00 USD Received 16 Mar 2015; revised 18 May 2015; accepted 19 May 2015; published 8 Jun 2015

surface stratification parameters

- R_k (core roughness depth) is the depth of the roughness core profile;
- R_{pk} (reduced peak height) is the average height of the protruding peaks above the roughness core profile;
- R_{vk} (reduced valley depth) is the average depth of profile valleys projecting through the roughness core profile;

amplitude parameters

- R_z (average maximum height of roughness profile) is the average height difference of the ten greatest peak-to-cleft separations and is calculated (Eq. (3);

$$R_z = \frac{1}{10}\left[\sum_{i=1}^{10} H_i - \sum_{j=1}^{10} L_j\right] \tag{3}$$

- R_p (maximum profile peak height of roughness profile) is the height of the highest peak from the mean line and is measured;
- R_v (maximum profile valley depth of roughness profile) is the depth of the deepest cleft from the mean line and is measured;
- R_t (total height of roughness profile) is the height between the deepest cleft and highest peak and is calculated (Eq. (4);

$$R_t = R_p + R_v \tag{4}$$

and characteristic average parameters

- R_{sk} (skewness of roughness profile) is the cube of the root mean squared absolute deviation from the mean line (R_q) and expresses the symmetry of peaks and clefts; skewness is calculated (Eq. (5);

$$R_{sk} = \frac{1}{R_{q^3}}\left(\frac{1}{l}\int_0^l Z^3(x)dx\right) \tag{5}$$

- R_{ku} (kurtosis of roughness profile) is the biquadratic of the root mean squared absolute deviation from the mean line (R_q) and expresses the sharpness of the roughness profile; kurtosis is calculated (Eq. (6).

$$R_{ku} = \frac{1}{R_{q^4}}\left(\frac{1}{l}\int_0^l Z^4(x)dx\right) \tag{6}$$

Of note, *surface stratification* parameters were derived from the construction of the Abbott-Firestone curve which is the cumulative amplitude distribution of the roughness profile calculated by its integration. By definition, the Abbott-Firestone curve is the ratio of the length of the bearing surface at any specified depth and hence synonymous with the surface bearing area ratio curve. Also, *cleft* will be used synonymously with *valley* in the following.

For correlation purposes, tissue protrusions, i.e. fibrillations, and tissue defects, i.e. clefts, were assessed on individual OCT images using ImageJ® software (National Institutes of Health, USA). To this end, tissue defects (Fig. 2(a), 2(g)) or protrusions (Fig. 2(d)) were identified and measured at their longest dimension in terms of depth (Fig. 2(b), 2(h)) or height (Fig. 2(e)), respectively, using the inbuilt rectangular selection tool. Respective depth or height was recorded in absolute pixel numbers. Wherever possible, up to five individual

#236329 - $15.00 USD Received 16 Mar 2015; revised 18 May 2015; accepted 19 May 2015; published 8 Jun 2015

structures representative of the image were measured and respective means calculated (Fig. 2(g), 2(h)). For the purpose of illustration, the detected surfaces (Fig. 2(c), 2(f), 2(i)) and corresponding primary as well as roughness profiles and underlying waviness are displayed (Fig. 3(a), 3(b), 3(c)).

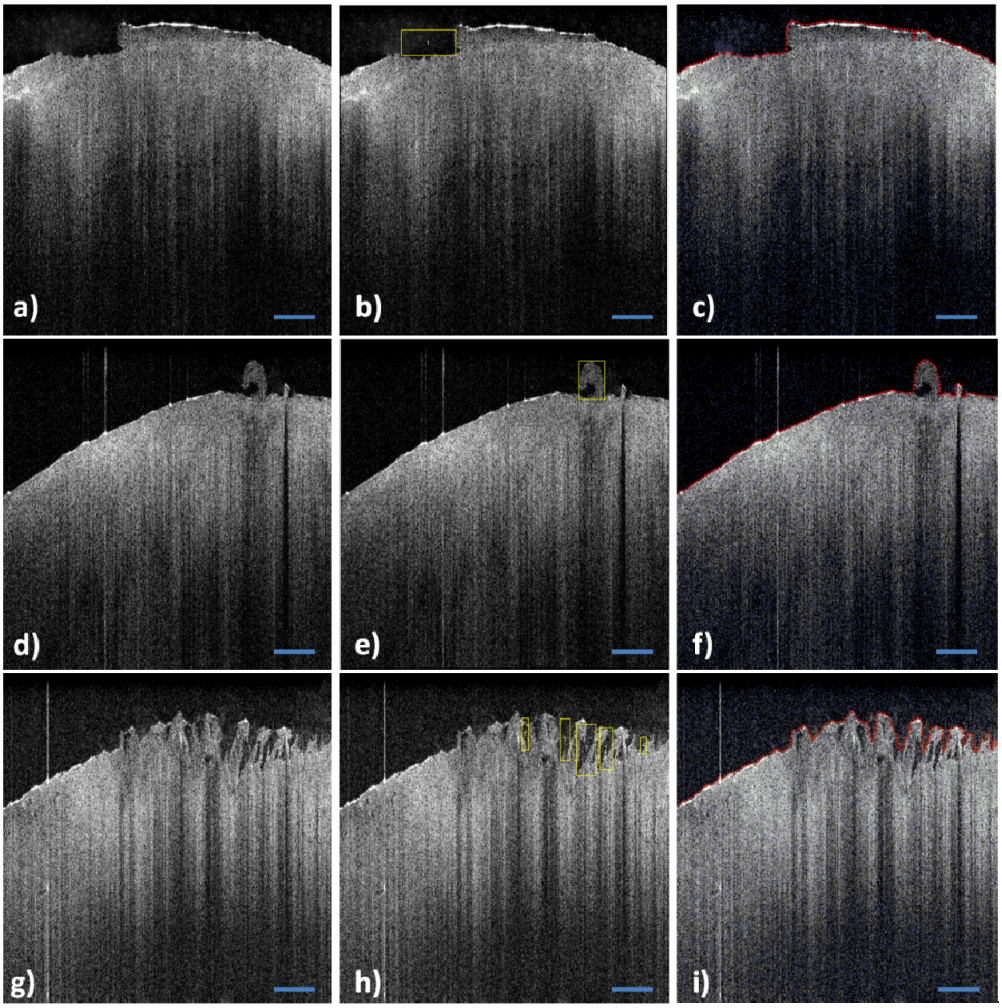

Fig. 2. Examples of manually quantified tissue surface features using ImageJ® software and algorithm-based surface detection and processing. Tissue defects (a, g) or protrusions (d) were identified and measured in their respective depth (b, h) or height (e) using the rectangular measurement tool provided. Up to five representative tissue features were measured per image (h). The red line marks the detected surface (i.e. primary profile, c, f, i). Bar represents 1 mm.

#236329 - $15.00 USD Received 16 Mar 2015; revised 18 May 2015; accepted 19 May 2015; published 8 Jun 2015

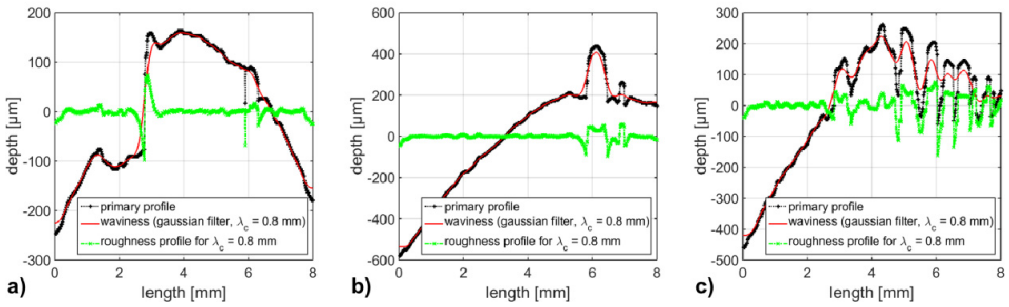

Fig. 3. The corresponding primary and roughness profiles as well as the underlying waviness of the human cartilage samples as displayed in Fig. 2. Here, Fig. 3(a)) corresponds to Fig. 2(a)-2(c)), Fig. 3(b)) to Fig. 2(d)-2(f)) and Fig. 3(c)) to Fig. 2(g)-2(i)).

Samples underwent routine histological analyses (i.e. decalcification and fixation in Ossa fixona (Diagonal, Muenster, Germany), sectioning along the imaging plane as defined above, embedding in paraffin, cutting to 5 µm sections and staining with hematoxylin/eosin and Safranin O). Histological image documentation was performed using a microscope (Leica DM LM/P, Wetzlar, Germany) and software (Diskus; same manufacturer). For histological analysis, a modified version of the DJD (Degenerative Joint Disease) grading system (equivalent to a surface-focused subcategory of Mankin Scoring [24]) as first published by Xie et al. [15] was used. Briefly, DJD 0 represents healthy cartilage, while DJD 1 denotes the presence of surface irregularities (i.e. wrinkling, fraying, laminar separations). DJD grades 2/3/4/5 are assigned to samples displaying cleft formation involving the superficial/transitional/deep/calcified zones, respectively. DJD grade 6 indicates complete loss of hyaline cartilage architecture (i.e. complete tissue disorganization, fibrous tissue replacement). Two blinded observers with experience in musculoskeletal histopathology performed histological grading (SL, SN). Of note, histological degenerative grading was considered the reference against which quantitative OCT-based roughness parameters were assessed and subgroup redefinition was performed.

Statistical analyses were performed using Graphpad Prism Software (Version 5.0, GraphPad Software Inc., US). Not assuming normal or linear distribution, correlations between histological DJD grades and individual roughness parameters were assessed using non-parametric Spearman's correlation coefficients. Kruskal-Wallis followed by Dunn's post-hoc testing was performed to assess differences between DJD groups after histological sample group redefinition. P-values ≤ 0.05 were considered statistically significant; more specifically [***] denote $p < 0.001$, [**] denote $0.001 \leq p \leq 0.01$ and [*] denote $0.01 \leq p \leq 0.05$. Likewise, correlations were classified and considered very strong / strong / marked / low / negligible with correlation coefficients $1.0 \geq r \geq 0.80$ / $0.80 > r \geq 0.60$ / $0.60 > r \geq 0.40$ / $0.40 > r \geq 0.20$ / $0.20 > r$, respectively.

3. Results

As outlined above, histology was considered the gold standard against which the quantitative OCT roughness parameters were assessed. After histological assessment, cartilage samples were graded as DJD 0 (n = 9), DJD 1 (n = 25), DJD 2 (n = 27), DJD 3 (n = 18), DJD 4 (n = 6), DJD 5 (n = 7) and DJD 6 (n = 13).

Average of ordinates parameters (R_a and R_q) and *surface stratification* parameters (R_k) demonstrated a close-to-linear degeneration-dependent increase with maxima found at DJD grade 5 (Table 1, Fig. 4). Although the overall trend was partially reflected by *associated surface stratification* parameters (R_{pk} and R_{vk}), R_{pk} values were about similar at DJD grades ≥ 4, while R_{vk} values were more heterogeneous overall. Similar to the global parameters above, *amplitude* parameters (R_z, R_p, R_v and R_t) displayed a close-to-linear degeneration-dependent

#236329 - $15.00 USD Received 16 Mar 2015; revised 18 May 2015; accepted 19 May 2015; published 8 Jun 2015

increase except for DJD grade 6. Similar observations were made for *characteristic average* parameters, in particular R_{sk}. While R_{sk} was negative in DJD grade 0 (i.e. the median value), its values steadily increased with increasing degeneration, except for DJD grade 6. No such trend was observed for R_{ku}, which was found to be in the range > 3 (3.068 - 4.086) throughout all DJD grades with slight increases noted in DJD grades ≥ 3. Overall, differences between all DJD grades (i.e. DJD grades 0 – 6) were significant for all parameters but R_{ku} (Table 1). DJD grade-specific pair-wise comparisons revealed a number of statistically significant inter-group differences, in particular between the DJD extremes, i.e. between DJD grades 0 and 1 vs. 4, 5 and 6, while no significant differences were found in several neighbouring DJD grades (i.e. DJD grades 0 vs. 1; 1 vs. 2; 1 vs. 3; 2 vs. 3; 2 vs. 4; 3 vs. 4; 3 vs. 5; 3 vs. 6; 4 vs. 5; 4 vs. 6; and 5 vs. 6) (Table 1).

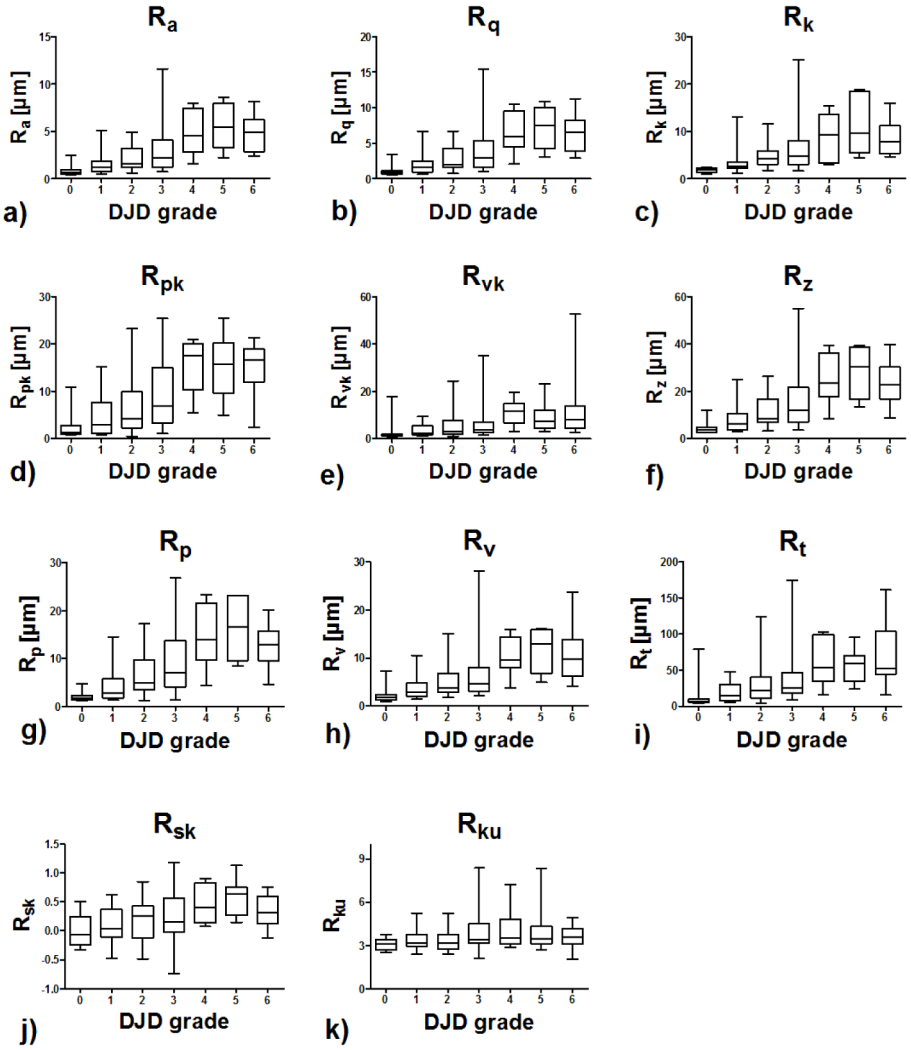

Fig. 4. Box plots of roughness parameters as a function of histological grading of cartilage degeneration (i.e. DJD grades). Medians are indicated by horizontal markers within the box plot, while boxes represent 25th to 75th percentiles. Whiskers (i.e. vertical markers outside the box plot) indicate the entire range of values. R_a (a), R_q (b), R_k (c), R_{pk} (d), R_{vk} (e), R_z (f), R_p (g), R_v (h), R_t (i), R_{sk} (j), R_{ku} (k). Of note, R_{sk} and R_{ku} are unit-less.

#236329 - $15.00 USD Received 16 Mar 2015; revised 18 May 2015; accepted 19 May 2015; published 8 Jun 2015

Table 1. Statistical analysis of degeneration-dependence of the roughness parameters plotted in Fig. 4. Differences between DJD 0 – 6 were assessed using the Kruskal Wallis test followed by Dunn's post-hoc testing. Significant differences are bold; more specifically [***] denote $p < 0.001$, [**] denote $0.001 \leq p \leq 0.01$ and [*] denote $0.01 \leq p \leq 0.05$. [ns] - non significant.

		R_a	R_q	R_k	R_{pk}	R_{vk}	R_z	R_p	R_v	R_t	R_{sk}	R_{ku}
DJD 0 - 6	p-value	**< 0.0001 (***)**	**< 0.0001 (***)**	**< 0.0001 (***)**	**< 0.0001 (***)**	**< 0.0001 (***)**	**< 0.0001 (***)**	**< 0.0001 (***)**	**< 0.0001 (***)**	**< 0.0001 (***)**	**0,0056 (**)**	0.4307
Dunn's post-hoc	DJD 0 vs 1	ns	ns	ns	ns	ns	ns	ns	ns	ns	ns	ns
	DJD 0 vs 2	ns	ns	**	ns	ns	ns	ns	ns	ns	ns	ns
	DJD 0 vs 3	*	**	***	ns	ns	**	**	*	*	ns	ns
	DJD 0 vs 4	***	***	**	**	**	***	***	***	**	ns	ns
	DJD 0 vs 5	***	***	***	**	**	***	***	***	**	*	ns
	DJD 0 vs 6	***	***	***	***	***	***	***	***	***	ns	ns
	DJD 1 vs 2	ns	ns	ns	ns	ns	ns	ns	ns	ns	ns	ns
	DJD 1 vs 3	ns	ns	ns	ns	ns	ns	ns	ns	ns	ns	ns
	DJD 1 vs 4	*	*	ns	**	*	*	*	*	ns	ns	ns
	DJD 1 vs 5	**	**	***	**	ns	**	***	**	*	*	ns
	DJD 1 vs 6	***	***	***	***	**	***	***	***	***	ns	ns
	DJD 2 vs 3	ns	ns	ns	ns	ns	ns	ns	ns	ns	ns	ns
	DJD 2 vs 4	ns	ns	ns	ns	ns	ns	ns	ns	ns	ns	ns
	DJD 2 vs 5	ns	ns	ns	ns	ns	ns	*	ns	ns	ns	ns
	DJD 2 vs 6	*	*	ns	*	ns	*	*	ns	ns	ns	ns
	DJD 3 vs 4	ns	ns	ns	ns	ns	ns	ns	ns	ns	ns	ns
	DJD 3 vs 5	ns	ns	ns	ns	ns	ns	ns	ns	ns	ns	ns
	DJD 3 vs 6	ns	ns	ns	ns	ns	ns	ns	ns	ns	ns	ns
	DJD 4 vs 5	ns	ns	ns	ns	ns	ns	ns	ns	ns	ns	ns
	DJD 4 vs 6	ns	ns	ns	ns	ns	ns	ns	ns	ns	ns	ns
	DJD 5 vs 6	ns	ns	ns	ns	ns	ns	ns	ns	ns	ns	ns

Individual roughness parameters were correlated to histological DJD grades (Table 2). Overall assessment of correlation (i.e. DJD grades 0 – 6) revealed strong and highly significant correlations for all parameters though being weaker for R_{ku}. When focusing on DJD grades 0 – 1, Spearman's correlation coefficient was highest for R_k, while the remaining correlations were significant yet weaker. R_{pk}, R_{sk} and R_{ku} did not significantly correlate. Correspondingly, when focusing on moderate-to-severe degeneration while excluding end-stage non-hyaline fibrous tissue samples (i.e. DJD grades 2 – 5), best correlation was found for R_p and R_z. Considerably weaker, yet significant, correlations were found for R_t, R_{vk} and R_{sk}, while R_{ku} was not significantly correlated. For all parameters but R_{sk} and R_{ku}, strong to very strong correlation to quantified individual tissue sample-specific tissue features was determined. Of note, best correlation was demonstrated for R_p and R_z.

#236329 - $15.00 USD Received 16 Mar 2015; revised 18 May 2015; accepted 19 May 2015; published 8 Jun 2015

Table 2. Correlation of roughness parameters to histological degeneration grades and to manually quantified tissue features. Degenerative stages are grouped as DJD groups 0 - 6 (n = 105), 0 - 1 (n = 34) and 2 - 5 (n = 58), respectively. Data are presented as Spearman's correlation coefficient (p-value [level of significance]).

	R_a	R_q	R_k	R_{pk}	R_{vk}	R_z	R_p	R_v	R_t	R_{sk}	R_{ku}
DJD 0 – 6	0.6748 (< 0.0001 [***])	0.6753 (< 0.0001 [***])	0.6982 (< 0.0001 [***])	0.6278 (< 0.0001 [***])	0.5343 (< 0.0001 [***])	0.6742 (< 0.0001 [***])	0.6746 (< 0.0001 [***])	0.6467 (< 0.0001 [***])	0.5854 (< 0.0001 [***])	0.3738 (< 0.0001 [***])	0.2115 (0.0304 [*])
DJD 0 - 1	0.4315 (0.0108 [*])	0.4315 (0.0108 [*])	0.5470 (0.0008 [***])	0.2344 (0.1820)	0.4519 (0.0073 [**])	0.4315 (0.0108 [*])	0.4247 (0.0123 [*])	0.4315 (0.0108 [*])	0.3975 (0.0199 [*])	0.1801 (0.3082)	0.1597 (0.3670)
DJD 2 - 5	0.4559 (0.0003 [***])	0.4643 (0.0002 [***])	0.4238 (0.0009 [***])	0.4431 (0.0005 [***])	0.3165 (0.0155 [*])	0.4920 (< 0.0001 [***])	0.5175 (< 0.0001 [***])	0.4500 (0.0004 [***])	0.3752 (0.0037 [**])	0.2963 (0.0239 [*])	0.1751 (0.1886)
Manual tissue feature size	0.8738 (< 0.0001 [***])	0.8755 (< 0.0001 [***])	0.8574 (< 0.0001 [***])	0.8432 (< 0.0001 [***])	0.7437 (< 0.0001 [***])	0.8810 (< 0.0001 [***])	0.8971 (< 0.0001 [***])	0.8416 (< 0.0001 [***])	0.8166 (< 0.0001 [***])	0.4525 (< 0.0001 [***])	0.2639 (0.0124 [*])

4. Discussion

The most important finding of the present study was that all relevant 2-D roughness parameters investigated were of distinct diagnostic value in the assessment of human cartilage surface integrity. Yet, considerable differences between *average of ordinates*, *surface stratification*, *amplitude* and *characteristic average* parameters were detectable.

Average of ordinates parameters (R_a and R_q) were found to display a close-to-linear degeneration-dependent increase with the peak at DJD grade 5 and a strong and highly significant correlation with histological DJD grades. These findings are in line with recent literature findings [17, 18] and may be due to proteoglycan depletion, secondarily decreased swelling pressure and increased mechanical wear due to degeneration [25]. Meanwhile, DJD grade 6 is marked by complete tissue disorganization and fibrous tissue replacement as a consequence of severe hyaline cartilage erosion and loss, which seems to be characterized by less surface roughness. As the above parameters allow the global assessment of the surface roughness profile, they are useful for detecting general variations in overall profile characteristics. Also, these parameters are well-established and understood in the technical characterization of surfaces. Mathematically, the influence of single irregularities such as peaks or clefts is limited in favor of stable results; hence, these parameters neither give information on the frequency or shape of irregularities nor do they distinguish between peaks or clefts or provide spatial structure information. Distinctly different surfaces characterized by either a sharp spike or a deep cleft can yield the same R_a and R_q value. In our study, both parameters essentially provided the same information which is due to their similar mathematical basis. However, R_q may be more sensitive to irregularities than R_a as the amplitudes are squared.

In order to assess the load-bearing capacity of cartilage, functional *surface stratification* parameters (R_k, R_{pk} and R_{vk}) were obtained using surface bearing area ratio curves. Similar to the global parameters above, R_k was found to be increased in relation to DJD grades and to be best correlated with overall (i.e. DJD grades 0 – 6) and early degeneration (i.e. DJD grades 0 – 1). On the whole, R_k as a global parameter may be most useful for the in-vivo arthroscopic cartilage assessment as the shape and dimension of surface irregularities (i.e. fibrillations, fissures) is dependent on local joint conditions such as fluid flow and pressure. As a measure of nominal roughness, R_k focuses on the running surface and limits the impact of anomalous peaks or clefts that may adversely affect measurement repeatability. On the other hand, R_{pk} and R_{vk} only partially reflected the degeneration-dependent increase observed for the parameters above. Overall, R_{pk} was better correlated throughout all DJD grades than R_{vk}, although no significant correlation was found for DJD grades 0 and 1. Besides, absolute R_{pk}

#236329 - $15.00 USD Received 16 Mar 2015; revised 18 May 2015; accepted 19 May 2015; published 8 Jun 2015

values were unchanged in moderate and severe degeneration (i.e. DJD ≥ 4), thereby limiting this parameters diagnostic sensitivity in higher degeneration, where fibrillations and fissuring increasingly undergo erosion. Therefore, this parameter may be useful for the characterization of functionally relevant protruding peaks in early-to moderate degeneration as it quantitatively describes the surface area functionally bearing weight. Correspondingly, due to the overall heterogeneity of parameter values and the inferior performance in comparison to R_k and R_{pk}, R_{vk} is a fairly limited roughness parameter and should therefore be only used as an adjunct to others.

Similar to the parameters above, *amplitude* parameters (R_z, R_p, R_v and R_t) displayed DJD grade-related increases and marked-to-strong correlations. Overall, these parameters were well correlated to both DJD grades and numerically defined tissue features. Consequently, these parameters may be useful for the evaluation of cartilage bearing and sliding characteristics that may be affected by protruding fibrillations or by debris-retaining clefts. As a global roughness measure, R_z may be more sensitive to surface changes than other global parameters, as it averages the ten greatest peak-to-cleft separations and thereby assesses maximum profile heights and not averages (as R_a or R_q).

Characteristic average parameters (R_{sk} and R_{ku}) included skewness describing the degree of skew, i.e. the symmetry of peaks and clefts, and kurtosis expressing the sharpness of the roughness profile. As above, analysis of either parameter revealed degeneration-dependent changes, although these changes were only significant for R_{sk}: A close-to-linear increase was observed for skewness with healthy cartilage close to zero indicating normal distribution, while samples with signs of degeneration (i.e. DJD ≥ 1) were skewed downwards relative to the mean line ($R_{sk} > 0$), indicating predominance of peaks. This parameter is highly sensitive to the dimensions of single irregularities (i.e. clefts and peaks) that have an impact of the third power, respectively, which helps to explain the degeneration-dependent increase. With more severe degeneration, tissue defects (i.e. clefts and fissures) become more pronounced [26]; interestingly, our data indicate that progressive degeneration involves more peak than cleft formation, at least in the context of roughness parameterization, which may possibly be due to overall tissue loss. Although highly significant, correlation with histological DJD grades was low by trend, thereby limiting the diagnostic relevance of skewness to a mere adjunct parameter. Likewise, the practical applicability of kurtosis is limited with only tendencies in differences detectable. While healthy cartilage surfaces are close to perfectly random ($R_{ku} = 3$), samples with signs of degeneration (i.e. DJD ≥ 1) are marked by increasingly variable and rather more pointed roughness profiles, in particular at DJD grades ≥ 3 ($R_{ku} > 3$). As above, this parameter is weakly correlated with degenerative stages and does not add significant diagnostic benefit.

Limitations of the present study involve the possible introduction of inaccuracy introduced by comparing OCT data to gold standard histology. Surface roughness was quantitatively assessed on OCT images by use of algorithm-based topography detection and subsequent parameterization and quantification of roughness, while histological images were graded qualitatively in terms of DJD grades. Hence, histological processing may have altered or distorted tissue structures, thereby affecting histological grading and subsequent subgroup definition. However, fixation and decalcification of the samples was performed using Ossa fixona®, which is a mixture of trichloracetic acid, zinc chloride and formaldehyde and widely established in orthopedic histology (e.g [27].). In line with other groups assessing cartilage surface roughness by means of histology [11], the authors are not aware that this procedure causes any changes to the overall surface characteristics although we concede that comparative evaluations (i.e. systematic surface evaluation before and after histological processing) have yet to be performed. Also, proper matching of OCT and histology cross sections proved challenging despite meticulous care paid to landmark and image plane definition. This may have introduced inaccuracy as cartilage samples are usually not uniform along their dimensions [28, 29]. Furthermore, the qualitative DJD classification as adapted for

#236329 - $15.00 USD Received 16 Mar 2015; revised 18 May 2015; accepted 19 May 2015; published 8 Jun 2015

OCT purposes relies primarily on the existence and dimensions of fissures and clefts. However, although cleft formation is a key component of cartilage degeneration, this complex cascade involves changes in cellularity and tissue functionality, morphology and composition. Analogous to the histological scoring of cartilage degeneration according to Mankin et al. [24], comprehensive OCT evaluation of cartilage should therefore also include the assessment of structural and optical parameters underneath the surface to make full use of the possibilities of OCT as a tomographic imaging modality that allows both surface as well as subsurface tissue assessment. In particular, the clinically relevant detection of early cartilage changes and their differentiation from healthy cartilage (i.e. DJD grades 0 and 1) was not sufficiently possible by stand-alone surface assessment. Therefore, more refined quantitative and depth-resolved approaches involving subsurface tissue properties need to be implemented to reliably differentiate all degenerative grades. Previous studies have suggested that combinations of surface and subsurface parameters are indeed beneficial in the comprehensive assessment of cartilage degeneration [16, 18, 19] as well as in cartilage-analogous in-vitro models [30]. More specifically, these studies have demonstrated a close interrelatedness of surface and subsurface parameters (i.e. optical backscattering and roughness [16]; optical homogeneity and irregularity [18]). As early degenerative structural and / or compositional changes may be present in cartilage tissue that seems superficially still intact [31], future studies should aim to further parameterize and quantify subsurface structural and optical changes that may be altered as a function of degeneration. These may involve refined techniques for the OCT-based detection of specific absorption- and backscattering-associated phenomena [32, 33]. Additionally, stand-alone surface assessment did not allow sufficient differentiation between a number of neighboring DJD grades, in particular in moderate-to-severe degenerative grades (i.e. DJD grade ≥ 3), while the differentiation between the DJD extremes was possible by the majority of roughness parameters. In this regard, the implementation of subsurface assessment strategies may improve the overall diagnostic performance of quantitative OCT. Another aspect to consider is the considerable parameter variability found in distinct DJD groups after histological group assignment. Specifically, roughness parameters of moderately degenerative samples assigned DJD grade 3 (and, though to a lesser extent, DJD grades 2 and 4) are marked by considerable statistical dispersion, thereby challenging histology-equivalent tissue grading by surface assessment alone. Accordingly, this particular degeneration-related variability may explain why significant differences were found when all DJD grades were assessed while less or no such differences were found upon pair-wise post testing.

To our knowledge, the present study is the first to systematically assess a representative set of OCT-based roughness parameters in the objective and standardized assessment of human cartilage while using a fully automated approach to determine the idealized smoothed surface used as a reference. This is in contrast to previous approaches as proposed by Chu et al. [13], Saarakkala et al. [17] or Cernohorsky et al. [19] that are characterized by requiring at least partial user input for reference definition. We consider the full automation of the underlying technical processes necessary to fit with surgical workflows when it comes to the actual clinical implementation of OCT-based surface parameterization and quantification.

In conclusion, the overall diagnostic performance of OCT-based cartilage surface assessment techniques may be further improved by using a combination of roughness parameters rather than a single parameter. As the roughness parameters investigated are distinctly different and their diagnostic strengths and weaknesses clearly related to the degenerative grade, a combination of well-performing *average of ordinates* (e.g. R_q), *surface stratification* (e.g. R_{pk}), *amplitude* (e.g. R_p) and possibly *characteristic average* parameters (e.g. R_{sk}) may provide a sensible approach to comprehensively assess cartilage surface changes. If a single distinguished parameter were to be chosen, R_k or R_z may provide valid alternatives to R_a and R_q. Future studies involving the actual in vivo or in situ setting are needed to further elucidate the clinical relevance of surface integrity assessment in the objective and standardized cartilage assessment by means of OCT.

#236329 - $15.00 USD Received 16 Mar 2015; revised 18 May 2015; accepted 19 May 2015; published 8 Jun 2015

Acknowledgments

This study was funded by the START program from the Medical Faculty of the University of Aachen, Germany, granted to SN. The study was in part supported by the Excellence Initiative of the German federal and state governments. Otherwise, the authors have no financial, consulting or personal relationships with other people or organizations to disclose. The authors would like to thank Ms. Sophie Lecouturier (SL) for performing the histological assessment and her overall technical assistance.

#236329 - $15.00 USD Received 16 Mar 2015; revised 18 May 2015; accepted 19 May 2015; published 8 Jun 2015